

Widely-Spaced Large Reflector Arraying for Space Surveillance

Ms. Kathleen Minear & Dr. G. Patrick Martin
Specialized Arrays Inc.

Abstract

The future of Space Domain Awareness (SDA) ground systems is widely-spaced, large reflector antenna arraying. Additional antennas can readily be added indefinitely to the array enabling it to ‘see’ further into space and at ultra-high resolutions. Space Force recently adopted large antenna arraying, as the enabling technology for the DARC program, a global GEO monitoring radar system.

NASA was the first to realize the benefits of arraying for Deep Space communications, funding three demonstrations between 2008 and 2010. Two significantly different approaches were created; one from government and the other from industry; Externally-Controlled and Self-Controlled, respectively. The Self-Controlled system does not rely on external satellites to repeatedly recalibrate it. If it’s powered up, it’s ready.

The government’s shift from fixed-sized to widely-spaced antenna arrays is logical. Fixed-sized antennas lack the ability to expand EIRP and G/T, limiting their reach and precision. The latest fixed-size antennas are Space Fence’s phased array and LeoLabs’ trough antennas. They are limited to LEO orbits, detecting objects that pass through a fan-shaped region of space.

Currently about 31,740 objects are regularly tracked internationally but there are estimated to be about 1,000,000 greater than 1cm², so a comprehensive approach was developed using a low-cost reflector array system, on or near the Equator, for instant high precision characterization of ALL Earth propagating objects.

The authors have spent the last 17 years demonstrating and inventing methods for widely-spaced antenna arraying for radar and COMM. As domain experts, we offer our insights, findings, and recommendations.

1. Introduction

Statistical models vary as to the number of Earth-orbiting objects that currently exist with ESA’s latest estimates being around 36,500 for objects greater than 10 cm, 1,000,000 between 1cm and 10 cm, and 130,000,000 between 1 mm and 1 cm [1]. Only about 31,540 are being regularly tracked, cataloged and maintained by Space Surveillance Networks. Of particular concern to space assets and astronauts are the 1-10 cm particles at altitudes up to GEO.

With this much debris circulating, self-generating collisions or Kessler Syndrome appear to be imminent with a crisis already brewing in low Earth orbit around 900-1000 kilometers. If this were to occur, space-based weather observations, climate monitoring, earth sciences, and satellite communications could be affected or lost [2]. Rural areas with limited ground infrastructure would feel the impact more.

Multi-stage shields, such as Whipple and variants, are effective for debris < 1 cm and are often used to protect key components of satellites and spacecraft, including the International Space Station (ISS) and the Space Exploration Technologies Corporation (SpaceX) Starlink satellites. Despite these shields, NASA says that, “millimeter-sized orbital debris represents the highest mission-ending risk to most robotic spacecraft operating in low Earth orbit [3].”

Objects > 1 cm are not mitigated by shields. The biggest threat to space assets is the 1-10 cm debris, with the highest risk being particles between 1 and 2 cm, demonstrated by the power law size distribution of explosive fragments [4].

Today's Space Domain Awareness (SDA) systems cannot effectively handle 1-10 cm size debris, which includes these 1-2cm high-risk threats, for two reasons.

1. They operate at S-band or lower
2. They lack the power and sensitivity to detect small objects beyond low Earth orbit (LEO)

One S-band example is the \$1.6 billion Space Fence, a large traditional phased array which came online in 2020. It is unable to characterize objects in this range. It can detect and characterize objects > 10 cm but doesn't have the power or sensitivity to detect them much beyond MEO.

Estimating using published data, Space Fence has 2.69 megawatts radiated power (36,000 elements at 74 watts each) and estimating the transmit array area from Google Earth, Space Fence, if it used its all of its transmit capability for a *single* beam, could realize a peak EIRP of about 122dBW overhead, but this rolls off at least as fast as $\cos(\theta)$, as it scans away from zenith.

Arrays of widely-spaced COTS ground reflectors are a solution to the small particle, high altitude problem. They are expandable by adding additional antennas, and so are able to provide the sensitivity and power needed for higher orbits like GEO. However, an array operating at X or Ka-band is required, not S-band.

Arraying at these higher frequencies is challenging and requires a reliable, robust arraying technology to keep the antennas synchronized. At Ka-band the phase errors are 3 and 10 times that of X and S-band, respectively. It also requires tropospheric mitigation since each antenna sees a different 'column' of the atmosphere. This causes a phase differential that needs correcting in real-time.

Despite the challenges, an X or Ka-band array could detect, characterize, monitor, and ISAR image particles at GEO as small as 10 mm or 4 mm, respectively (assuming RCS is full optical size), if the orbit determination method utilizes the wide diameter of the array for high precision steering vector angle of arrival calculations. (Fig. 1).



The enabling technologies for this system are

- “Self-Controlled” arraying methodology
- Tropospheric mitigation

Both were successfully proven¹ at X-band during an industry-led, NASA-funded program, program TxACE² [5][6]. During the 10 months of operation, the array produced an optimal beam, never needing calibration.

This technology has been further developed, by the authors, over the last decade to work at higher frequencies, like Ka-band, and for radar space domain awareness applications [7].

Current arraying state of the art is found in Section 2. What it takes, sizing the system, is presented in Section 3. Two

methods for arraying are discussed in Section 4. An arraying demo overview is in Section 5. The Self-controlled arraying solution and results are in Section 6. A brief history of arraying experiments is in Section 7. Valid performance metrics are in Section 8 and a conclusion in Section 9.

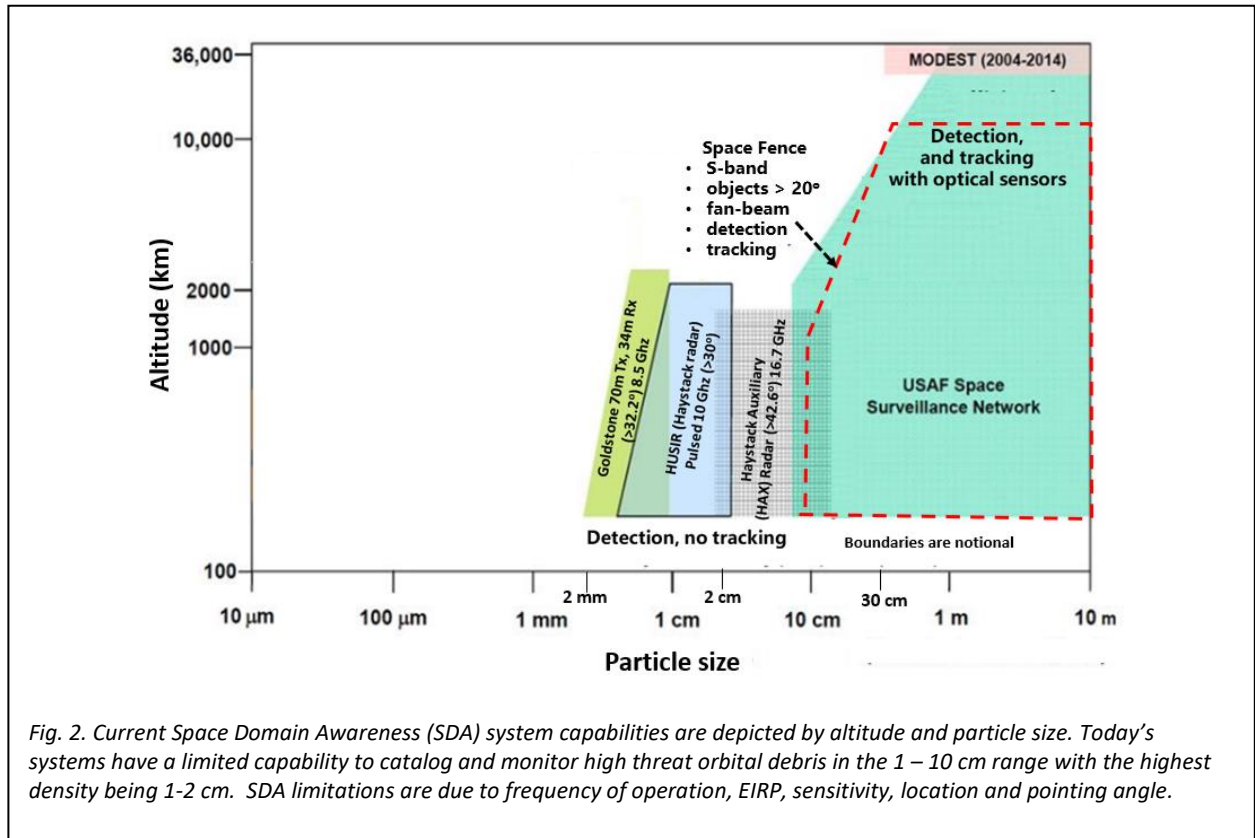
¹ Martin and Minear, Exceptional Engineering Achievement Medals, 2011, NASA HQ by former Administrator. Maj Gen Charles Bolden and former NASA Associate Administrator Dr. Christopher Scolese

² Transmit Antenna Combining Experiment 2008-2010 in Palm Bay, Florida, led by Martin & Minear

2. Current Space Domain Awareness system capabilities

Today's systems are unable to detect small objects at high altitudes due to frequency of operation, aperture size, sensitivity, power, location, and orientation. They are also limited with respect to object inclinations.

Holding up progress is the notion that the solution to orbital debris cataloging is to increase the number of systems that search the vastness of space; either passively, by making fan-beams and waiting for arbitrary objects to fly by, or actively, by scanning the sky in particular regions of interest. While the problem is growing, systems continue to go down this path. Fig. 2 shows current system capabilities by particle size and altitude³.



While S-band are able to detect objects down to 2 cm, they lack the power and sensitivity to do so at high altitudes. The 1–2 cm range poses the greatest threat and requires an X or Ka-band (8-32 GHz) system which can detect 6 mm and 2 mm objects respectively by using a wide diameter reflector array and specialized algorithms. A system designed with sufficient EIRP and G/T would enable object detection and cataloging at high altitudes, like GEO.

This led to the development of ESSAR in 2014 - 2018⁴. It is a notional, one-pass Equatorial radar system, using a horizon pointing stare-mode, that can comprehensively detect and catalog *all*, propagating, Earth-orbiting objects due to the properties of its unique location and orientation, within 10 degrees of the equator and horizon pointing. A modification was also developed and also patented that handles non-propagating object, in geosynchronous orbits.

In the figure near the lower middle, there are three systems that are able to detect but not track objects. They include Haystack (10 GHz), Haystack Auxiliary (16.7 GHz), and Goldstone (8.5 GHz). On the right, the red dashed box

³ Figure credit: Modified from the IARPA proposer's day presentation

⁴ Patented, ESSAR: Equatorial Space Situational Awareness Radar

represents Space Fence. It is a traditional phased array, limited to larger object sizes since it operates at S-band and has insufficient EIRP and G/T to handle higher orbits.

The cyan region represents the Space Surveillance Network optical telescopes which are able to detect and track objects in their field-of-view. However, due to sensitivity limitations, the minimum sizes maintained in the space catalog are about 70 cm in GEO and 10 cm in LEO.

The boundaries are notional with the particle size limit determined by the frequency of operations and the altitude limited by the power and sensitivity of the system. The inclination angle of objects that can be detected is affected by the system location, orientation, and overall hardware design.

Fig. 3 shows the altitude and particle size coverage region for a notional X-band COTS large reflector antenna array. System parameters were selected to at least cover particle sizes 1-10 cm up to GEO. Selected parameters include: 36 12m COTS reflectors for the Tx and Rx arrays, Objects $\geq 0^\circ$ inclination, Location: Equator, HPA: 10kW, Frequency: 10GHz. A detection SNR of 20dB up to GEO is specified in order to obtain good AOA, so smaller or more distant objects can be detected with reduced orbit determination precision.

It appears possible to get down to 2 mm object sizes at GEO using 36 12m reflectors at Ka band, but requiring a 20kW HPA. Only about 1.2kW is COTS at present.

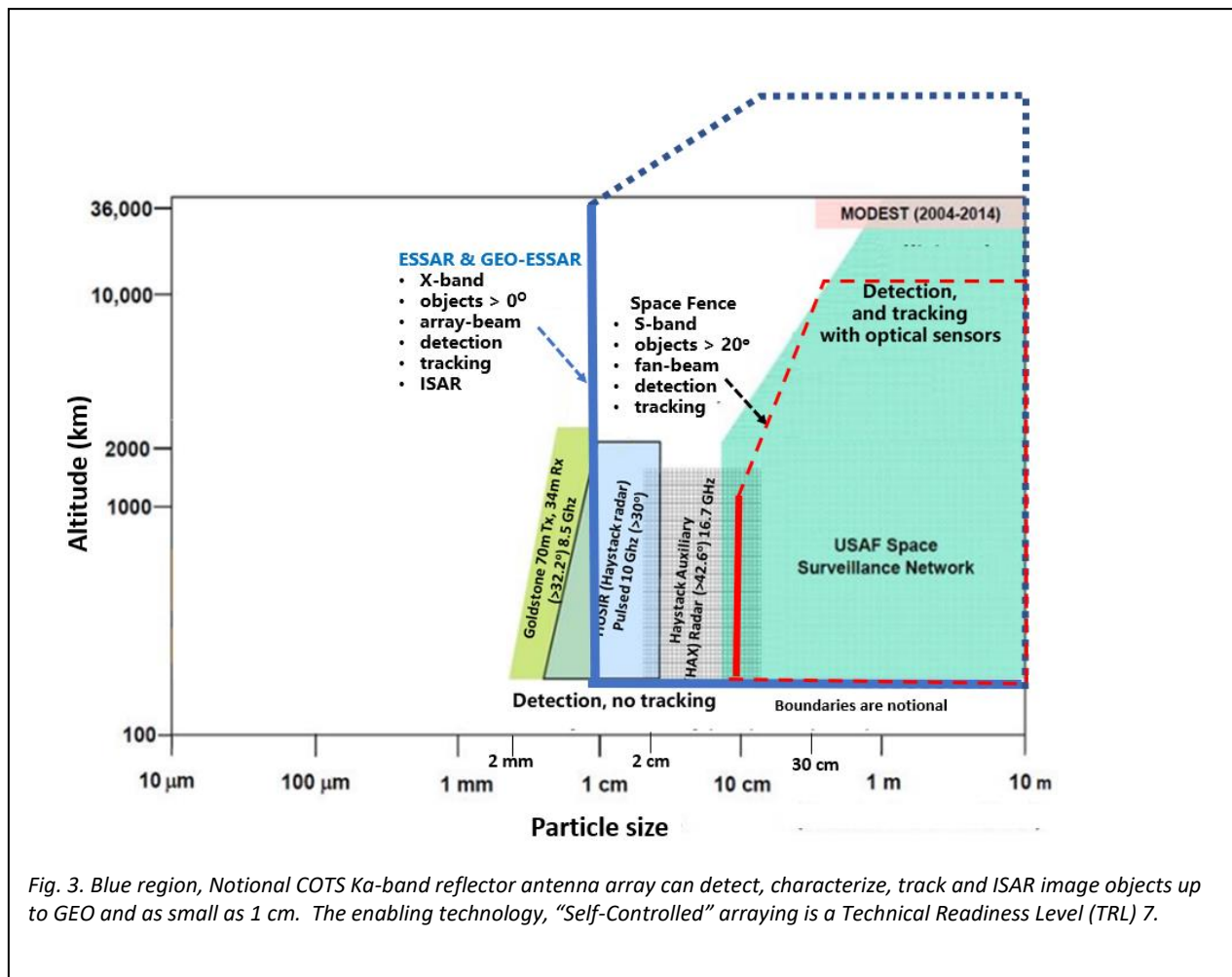


Fig. 3. Blue region, Notional COTS Ka-band reflector antenna array can detect, characterize, track and ISAR image objects up to GEO and as small as 1 cm. The enabling technology, "Self-Controlled" arraying is a Technical Readiness Level (TRL) 7.

3. What it takes

This is a formidable challenge; one intends to detect and determine the orbit of a marble-sized object 36,000 km or more distant. The object's orbit needs to be determined when it is detected, since minutes later, that object might be confused with another similar object. Consequently, methods depending upon multiple observations over an extended period of time, like those used for large objects, are not applicable.

The design could be applied in a quasi-staring scanning process, so as to include geostationary and geosynchronous objects. However, we note that with an array location on or near the equator, eventually all propagating objects will pass through an equatorial plane staring beam. Three equatorial X-band systems like this could, on average, 'see' everything 1cm or larger in less than one year, appreciating that changes in the population are not dynamically updated.

3.1 Detection and Orbit Determination

This discussion is focused on objects at or near GEO. Waveform and/or processing changes are required for operation at LEO altitudes. If only LEO or MEO is of interest, a much smaller array design would result; possibly a subset of the larger system.

An orbit can be determined from an object's 3D position and velocity. This information can be obtained from a monostatic radar array using two (or more) successive measurements. With respect to the array's phase center, the returned echo can be processed to yield the object's range and range rate (line-of-sight velocity). Additionally, using the array's Angle of Arrival (AOA) capability, one can also obtain 2D cross-range, collectively yielding the object's 3D position. With a second observation immediately afterwards, cross-range differentials yield cross-range rates (cross-range velocity). These observations from the coordinate system aligned with the array boresight can then be transformed into any convenient coordinates, for example, ECEF (Earth Centered Earth Fixed). Since these measurements are taken sequentially, it is highly likely they are from the same object.⁵

With focus on a monostatic array, wide element spacing is necessary for precise AOA (angle of arrival). Ideally, one would want cross-range resolution to be commensurate with range resolution (determined by the transmitted waveform bandwidth and achievable S/N). For range resolution of a few meters, a waveform bandwidth of more than one hundred MHz is needed. For cross-range resolution of the same few meters, for example, 3m at GEO, the array's Diameter measured in wavelengths must satisfy

$$R_{GEO} \left(\frac{\lambda}{D_{Array}} \right) (split) \approx 3$$

Where $(split)$ is the array's AOA algorithm ability to resolve a fraction of the array beamwidth. For example, Monopulse typically achieves a beam split factor of 10% while Steering Vector AOA can realize 1% to 2% (1/100 to 1/50 beamwidth) depending upon S/N. Let us assume the array is in an aperiodic configuration within a D_{Array} of about 1.2Km. Assuming a 1% split, we see that the array frequency would need to be 30GHz, or Ka band. At X band frequencies, this same array could obtain about 10m cross range resolution at GEO.

If the objective is to detect and determine the orbit of objects as small as about 10mm in size (diameter), an X-band frequency is needed in order to be above the Rayleigh scattering effect where an object's RCS diminishes as the fourth power of size when the object's circumference is less than a wavelength, see Fig. 4.

⁵ A multistatic configuration of at least three non-colinear arrays could obtain range and range rate simultaneously in three or more independent directions, and thus an orbit in one pulse

From the graph, RCS is down by 0.5 (or 3dB) when the circumference is 1/2 wavelength. At 10GHz, the wavelength is 3cm, so the object diameter d would be given by $\pi d = \frac{1}{2} 0.03m$. So, an object of about 5mm diameter, half the size of our 1cm objective (marble size) should be within scope.

$$d = 0.03 / (2\pi) = 4.8mm$$

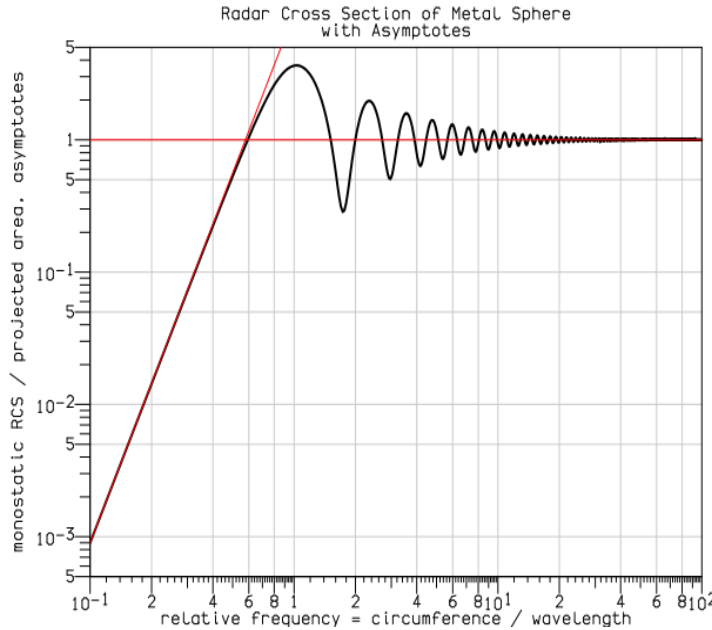


Fig. 4. Radar cross section of a metal sphere vs relative frequency; particles at the design diameter of 10 mm appear to be larger than optical size

3.2 EIRP and number of elements

We may use the following array radar equation to nominally size the array

$$SNR = \frac{N^3 P_a A_e^2 f^2 \sigma}{k T_s B (4\pi c^2) R^4}$$

Where f is frequency of operation, c is the speed of light, R is range from the radar to the object of interest, σ is the effective cross section of the object (area) which intercepts the radar transmission and is assumed to scatter isotropically. B is processing bandwidth (inverse of the waveform integration time τ), T_s is the system temperature of the array when receiving, and k is Boltzmann's constant. Antenna effective area A_e , and likewise the associated gain G_e , includes antenna efficiency, η .

It is notable that the received SNR is proportional to the number of array elements cubed (assuming the same number of elements is used for both transmit and receive). A factor of N squared is obtained for transmit, since directivity increases by N and transmitter power P_a is also independently provided at each element, giving a combined factor of N squared. Receive array gain increases as N , so the radar two-way performance is proportional to N cubed (or $N_{TX}^2 N_{RX}$).

If we specify a certain SNR for detection and AOA determination, then we can rearrange the equation to solve for the number of antennas required. One has

$$N = \sqrt[3]{\frac{kT_s B (4\pi c^2) R^4 SNR}{P_a A_e^2 f^2 \sigma}}$$

We will take $R = 36,000\text{km}$ while requiring $SNR = 20\text{dB}$ (for precision AOA). RCS $\sigma = -41\text{dBsm}$ (~10mm diameter objective). HPA power 10kW is available at $f = 10\text{GHz}$, and with LNA cryogenic cooling and a high-altitude location for the array, a system temperature of 35K should be possible. COTS 12m reflectors, 70% efficient, with good performance at X band are relatively inexpensive and readily available. We set system bandwidth B to 4Hz, allowing for round trip time to GEO. With these parameters, an array with 36 12m reflectors results.

Interestingly, with an available 30GHz 1.2kW TWT HPA and the same 36 reflectors, a 2mm object at high MEO (16,000km) is detectable.

This notional array sizing implicitly and naively assumes that the number of transmit and receive elements are equal, or even that the same elements could be used for both transmit and receive. In some applications, this may be a viable option, but in an SDA application there are compelling reasons for having separate transmit and receive arrays, each with customized lattices even though this option significantly increases the number of elements required (double, with the present assumption).

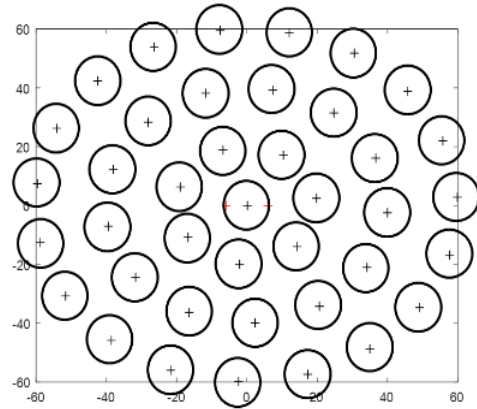


Fig. 5. Example of an aperiodic lattice of 40 12m reflector antenna and a diameter of about 120 m

As discussed earlier, for good angular resolution, the receive array needs to be widely spaced. This will result in an antenna pattern with many lobes, requiring potential grating mitigation. Such a pattern is not desirable for target illumination; instead, a tightly spaced array with minimum lobing is preferred.

Potential grating can be mitigated if both of these lattices are aperiodic, largely ensuring that lobes in one do not coincide with lobes in the other. This improves two-way radar performance against ambiguous targets. (At least three other techniques for potential grating mitigation are known, but this topic is beyond the scope of this paper.) An example of a tightly spaced aperiodic lattice with 40 12m reflectors within an array diameter of about 120m is given in Fig. 5 at X band, this results in a 9km diameter spot size at GEO. A particle in a worst-case retrograde GEO orbit would traverse this spot in about three seconds, allowing for up to 12 successive radar pulses. (At Ka band frequencies and this same lattice, the transmit beam diameter at GEO would be about 3km.)

3.3 Critical considerations

While the atmosphere is relatively benign at S-band, it is noticeably variable at X-band, especially in stormy weather, and highly variable at Ka-band, even under seemingly ideal weather conditions. Tropospheric instability was studied by Glenn Research Center, in 2010 as a result of a proposed Ka-band antenna array, using White Sands, (WS)⁶ and Goldstone⁷ sites and setting up atmospheric phase monitors using a two-element interferometer [8]. Tens of degrees phase change over intervals of seconds were observed.

This means that without real-time tropospheric compensation for individual array elements, accurate transmit beam formation and accurate AOA is impossible. We demonstrated this at X-band with 3 12m antennas. Section 6.3 explains how this was done.

⁶ White Sands Tracking and Data Relay Satellite (TDRS) Complex

⁷ Goldstone DSN Complex, near Barstow, California

4. Reflector arraying: two methods

Whether the array of reflector antennas will be used as a radar for orbital debris, communications to a Mars colony, resilient comm through nuclear disturbed environments, beyond-line-of-site comm, or high-powered directed RF energy missions such as electronic warfare, unless the array of antennas can seamlessly behave as though the signal emanated from a single antenna, mission failure is likely.

To date, there are two distinct, demonstrated methods for synchronizing the widely-spaced large ground reflectors.

1. Externally-Controlled (uses satellites or towers)
2. Self-Controlled (uses local 100% phase lock)

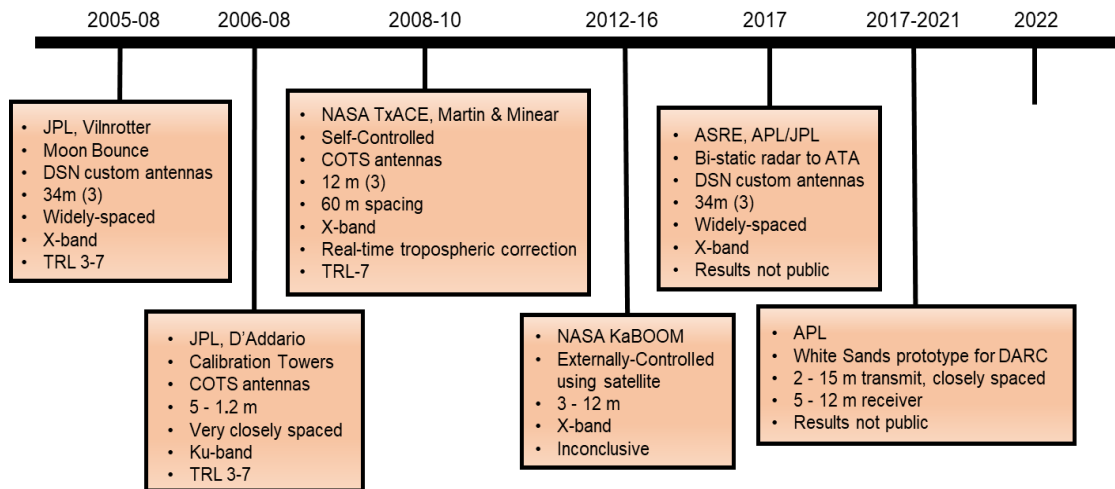


Fig. 6 From 2005-2016 NASA funded several arraying technology demonstrations. All except one (TxACE) used variations of the Externally-Controlled arraying method. TxACE was the only industry-led arraying demonstration taking place in Palm Bay, Florida, 2010. It used Self-Controlled arraying technology.

From 2005-2016, NASA funded several experiments that used the Externally-Controlled arraying method, all involving JPL as shown in Fig. 6. Externally-Controlled arraying relies on external sources. The Moon, towers, and satellites were all tried. Lacking a 100% phase lock on the system, each time the antennas drifted out of calibration these external sources needed to be used to realign them.

The first experiments that used at least three antennas were Moon Bounce and Calibration Tower methods. The tower method was only applicable to small antennas since the towers needed to be in the far field of the array. For large reflector antennas, like KaBOOM, a GEO satellite replaced the tower.

4.1 Externally-Controlled arraying (JPL)

This method was influenced by a JPL 2003 paper by Amoozegar, et al [9] and subsequently copied by other national laboratories such as APL and MIT-LL. In the 2003 paper they provided an argument for external calibration that persists until now in the section titled, “Why Calibrating with Moving Targets in Earth Orbit”.

The argument basically asserts that only observation of far-field objects can provide the information needed to account for antenna and circuitry phasing errors among the elements of the array. An alternative architecture that phase-locked the entire system, such as Self-Controlled arraying was not considered at that time.

4.1.2 Main features

The main feature of Externally-Controlled arraying is the inherent use of external objects such as satellites, towers or the Moon in the arraying architecture. Because some of the hardware and antenna components are not phase

locked, the array will drift out of calibration and an external object is used to provide the feedback needed to recalibrate it.

4.1.3 Main drawbacks

With this method, there is always an unknown phase in the excitation of every antenna, and this must be determined using feedback from an external far-field known source before a coherent beam can be formed. Between calibration events, the state of the system is unknown. As the system drifts out of coherency, mission performance deteriorates, often very quickly.

Additionally, lack of precise orbit information for the calibration target will unknowingly, add to the calibration errors. This method often relies on partial control loops, and temperature stabilization of, as much of the electronics and fiber as possible. Line stretchers can be implemented in these partial control loops. These mechanical devices reach hard limits causing the system to stop and reset.

The length of time this method remains coherent is limited, unknown, and a function of the frequency of operation and distance between the antennas. This method is unable to operate at higher frequencies since unknown propagation variation prevents good calibration and prevents continual real-time correction of propagation media variation.

4.2 Self-Controlled arraying (Martin & Minear)

During 2008 – 2010, NASA funded TxACE, Transmit Adaptive Combining Experiment [10]. This method challenged and disproved the assertion that a known far-field object was necessary for array calibration. It appreciated that fundamentally the calibration problem can be factored into two components:

1. The antennas and their locations,
2. The associated electronic circuitry connecting and controlling them, including the antennas

These components can be addressed individually. Both Externally-Controlled and Self-Controlled arraying methods require the first component.

A third error contributor is not one of calibration per se, but one of propagation media variation. With the first two components addressed for *both* transmit and receive arrays, it is optionally possible to measure and adaptively correct for environmental disturbances. This added feature enables reliable operation at X and Ka band as well as resilient communications in disturbed environments. It was demonstrated in 2010, achieving TRL 7, and the authors received Exceptional Engineering Achievement Medals from NASA June 13, 2011.

4.2.1 Main features

The Self-Controlled method addresses all electronic variation by placing the entire array, all hardware, fiber, and antennas, in a vectorial phase-locked loop. Sensors on each antenna surface sample the transmitted signal at the last accessible point before the wave is radiated, providing feedback necessary to control the entirety of array circuitry to zero mean phase error. Ordinary COTS hardware can be used since its phase variation is within the control loop. Custom, well known and controlled, state-of-the art antennas, like those in the DSN are not needed.

Within milliseconds after power up and for as long as the array is operating, the array is calibrated, see Fig. 7. The receive array is similarly calibrated.

As an optional benefit to the 100% phase lock on the receive antennas, any known location source of arbitrary frequency within the element pattern's main beam at that frequency can serve to real-time probe the propagation media. Deviation between the measured and expected source steering vector quantifies propagation variation due to media disturbance; frequency scaling the deviation then enables tropospheric pre-correction of the transmit beam.



Fig. 7: If it is on, it's ready – Self-Controlled Method

4.2.3 Main drawback

Not owned by the government. The 2010 demonstration was an industry-led, NASA-funded project with the authors, the principal investigators. During the program key arraying components were designed and built, the technology was reduced to practice. In 2011 the antennas and the phase-lock critical sub-component were delivered to NASA Kennedy Space Center, (KSC). The KSC/JPL team reverted to the more familiar Externally-Controlled arraying method during 2012-2016.

5. Overview of arraying demonstrations

In 2009 NASA funded an arraying study at JPL [11]. Five small 1.2 m antennas were arrayed at 14Ghz and the target was a commercial satellite. While it was a communications demonstration, it featured arraying, the same enabling technology required for an orbital debris radar system, like DARC. The system was not 100% phase locked so calibration towers were used to calibrate or synchronize the antennas. Despite the very close spacing of the antennas, unknown phase errors caused by filters, antenna feeds, amplifiers, and the antennas themselves, caused the array to drift out of calibration, losing about 1dB over 3 days [12]. To continue operations, recalibrating with the towers would be required.

Fig. 9 and Fig. 10 and show the five JPL antennas. Because the 1.2 m antennas were very close together, antenna-to-target tropospheric variations were not likely the biggest error contributor to the phase drift, but rather the arraying methodology, Externally-Controlled arraying. For a *widely*-spaced array at the same frequency, 14Ghz, the inhomogeneous distribution of water vapor would cause the array beam to deteriorate quickly.

We showed this phenomenon at X-band with 3-12m antennas, 60 meters apart in 2010 [13]. In that demonstration, tropospheric variations among the widely-spaced antennas required real-time tropospheric mitigation adaptive algorithms, particularly at low pointing angles and during weather events. Goldstone experiments by NASA Glenn Research Center, also confirmed this well-known phenomenon by observing unmodulated beacons from a geostationary satellite using a two-element interferometer spaced 256 m apart at 20.199 Ghz at an elevation of 48.5 degrees [14].

Fig. 8 shows two closely-spaced transmit reflector antennas at White Sands (WS). In 2021 APL conducted an arraying experiment before turning the arraying technology over to Space Force for the DARC program. “DARC builds on a 2009 study conducted by NASA to explore how an array of small antennas can serve as a lower-cost alternative to a single large antenna [15].” Counterweighted electronics in the back functionally resemble the 1.2 m 2009 system. To augment the SSN, Space Force intends to build a very large reflector antenna system on multiple sites. Each site would have 10-15 large reflector antennas for the receive array and 4-6 for the transmit array covering about 1km square [16]. Site one was recently won by Northrop Grumman. The goal is to provide an all-weather, 24/7 capability for GEO asset monitoring. Completion is expected in 2025 in the Indo-Pacific region [17].



Fig. 9 2009 NASA JPL array study Left side counterweight carries DC power supplies for the electronics



Fig. 10 2009 NASA JPL array study, 5 1.2m offset paraboloid antennas “Calibration Tower Method”



Fig. 8 2020 APL White Sands closely-spaced transmit antenna array setup; DARC technology

From 2012 – 2017, NASA funded another externally-controlled arraying experiment at KSC under the names KaBOOM and later KARNAC. Despite the names, it was an X-band, not Ka-band experiment. (Fig. 11) Unlike the 2009 Calibration Tower experiment, the antennas were larger, 12m, so the calibration source needed to be further away in order to be in the far-field so a GEO satellite replaced the calibration towers. The arraying method had the same limitations as the 2009 experiment, antenna drift between calibration events, due to the uncontrolled hardware. With antennas 60m apart, the effects were much more significant [18]. They attempted to fix those effects.

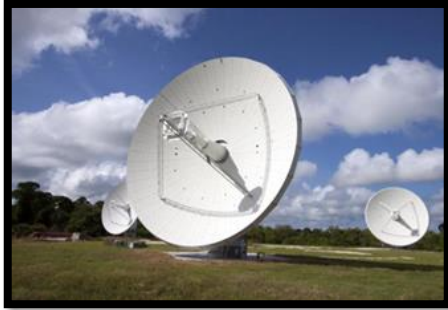


Fig. 11: Externally-Controlled arraying, NASA KSC, KABOOM/KARNAC, X-band experiments

The final KSC KaBOOM paper from this effort does not support the assertion, “NASA has successfully demonstrated coherent uplink arraying with real time compensation for atmospheric phase fluctuations at 7.145-7.190 GHz (X-band)”. Pages 4 and 5 of the paper are devoted to experimental results supporting this assertion. Two sets of data are presented, dated Jan 15, 2016 and June 7, 2016. These are presented in pairs, respectively with the legends, “Correlation On” and “Correlation Off”. The title of a graph on page 4, a two-antenna experiment, reads “Jan15 xcor ampl 1-3”, apparently inferring the real part of the complex correlation between receive array antennas 1 and 3. Similar data are presented on page 5, but pairwise receive correlation

respectively for 1-2, 1-3, and 2-3. No algorithm is presented, but it is stated, “The idea was ... to see ... whether the cross-correlation phase could be used to correct the uplink phases.”

However, it must be noted that the ‘improvement’ cited in receive array cross correlation standard deviation is unrelated to transmit array phasing correction (which produces a single signal at the satellite). This signal received by the satellite is the sole, scalar, measurement of the transmitted beam quality. A measurement of that signal was not reported in this paper. Such an improvement would necessarily be shown by a bent pipe downlink of the scalar transmit signal received by the satellite, not cross correlation of receive array signals. Consequently, the data presented in this paper do not support the assertion of successful compensation of atmospheric phase fluctuations.



Fig. 12 Self-Controlled arraying, only industry-led government-funded arraying demonstration

From 2008-2010, on the only industry-led NASA funded array demonstration, 100% array phase lock and real-time tropospheric mitigation were successfully demonstrated. (Fig. 12) The 3-12m X-band antenna array remained calibrated for a 10-month period without the external assistance of towers or satellites. This is called the Self-Controlled method. Each time it was powered up, it was coherent, never needing recalibration. Details on this method will be discussed in the next section.

6. Self-controlled arraying method explained and results

There are three principal error contributors in arrays of large reflector antennas

1. Imprecise knowledge of the geometrical factors needed to determine time of flight and phasing from an antenna’s phase center to the distant target
2. Circuitry variation between the point where a signal is phased for transmission and the location from which that signal is radiated or received
3. Uncompensated differential propagation phase variation caused by tropospheric effects

5.1 Geometrical factors

Whether Self-Controlled or Externally-Controlled arraying methods are applied, precise geometrical knowledge of the antennas and their positions is necessary in order to calculate beamforming parameters in an array model. Given ideal antennas, the surveyed antenna reference point, ARP, 3D location (usually the intersection of azimuth and elevation axes) satisfies this need. However, with real antennas, one must account for other factors including center of rotation variation, surface distortion, subreflector positioning and alignment. Since beamforming time delay and phase vary with pointing, these geometrical/mechanical parameters in the array model must be correct, since clearly a single calibration value for each element cannot correct a pointing dependent functional variation.

Positional errors become more important as element spacing increases, since these cannot be corrected with a single calibration measurement.

It is notable that the Externally-Controlled method is more sensitive to geometrical or mechanical errors, since these errors count twice: first by biasing calibration measurements, then again in beamforming calculations. In the Self-Controlled method, they only occur during beamforming.

5.2 Circuitry variation

Circuitry variation is the principal source of error in widely spaced arrays. Typical circuitry includes not just fiber-optic transmission lines, but upconverters, filters, fiber-optic transmitters and receivers, and power amplifiers. All of these components are temperature sensitive and time variable. Circuitry variation over time and temperature is the dominant error in beam formation at X-band, and distributing precisely phased signals to the antenna elements becomes increasingly difficult as separation and frequency increase.

Circuitry variation is often addressed by stabilization of the most sensitive components, such as fiber transmission lines. However, all of these methods are characterized by a residual unknown phase at each element that must be determined using a known external calibration target. In high powered transmitters, this unknown phase component is typically the HPA and temperature sensitive antenna circuitry, such as waveguide filters.

In the Self-Controlled method, all components, including transmission lines, frequency converters, filters HPA, and the antenna itself including the feed with polarizer and filter are placed in a vectorial phase-locked loop. Consequently, there is no unknown phase and any potential phase drift is instantly corrected. In practical terms, the circuit contribution to the array's beamforming error is zero.

This method has other advantages. The array is always ready for operation, not dependent upon external objects availability or calibration process errors, and permitting failed component replacement without the need for recalibration.

Fig. 13 conceptually illustrates this method. Both receive and transmit pathways are controlled, but we will focus on the right-hand side transmit pathway (shown in red). A required precise phase reference at widely separated physical locations can be implemented with two-way time or phase transfer.

At a point including as much circuitry as feasible, a sample of the transmit signal is compared with the remote phase reference, similarly at the point of generation. Any phase deviation in the comparisons can be attributed to circuit

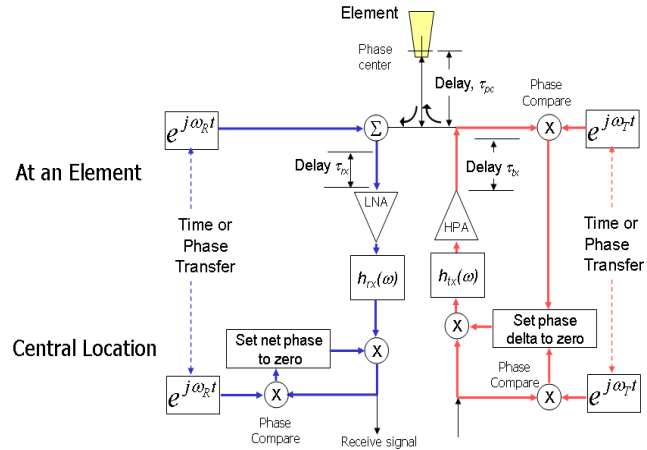


Fig. 13. Self-Controlled arraying technology conceptual diagram

variability. A weighting device in the transmit pathway applies the measured correction, forcing the entire pathway to zero phase shift between generation point and transmission.

Fig. 14 illustrates how the feedback point can be located on the reflector surface, thus including all temperature sensitive feed components and internal reflector variation as well as the HPA and cable wraps. This is the last accessible physical point before the wave leaves the reflector. As the reflector and its components expand and contract due to temperature changes, the circuit path length change is sensed and corrected.

Fig. 15 shows a field sensor installed on one of the 12m TxACE reflectors. Error detection hardware is mounted just behind the surface.

In this way, all unknown circuit phase errors can be sensed and controlled, making the antenna ready for instantaneous optimum transmit operation.

In addition to negligible latency, immediate availability and no point-away requirement, this method is relatively low in cost since ordinary COTS hardware can be substituted for precision, temperature stabilized components. Transmission lines need not be environmentally controlled. Since time delay compensation is accomplished at baseband, only approximate delays are needed to satisfy time*bandwidth constraints (RF transmit phase is unaffected). This approach applies to arrays of any size and is particularly well suited for array expansion. Since each array element is independently ready for service at any time, partitioning a large array into subapertures (such as 34m equivalents) is straightforward.

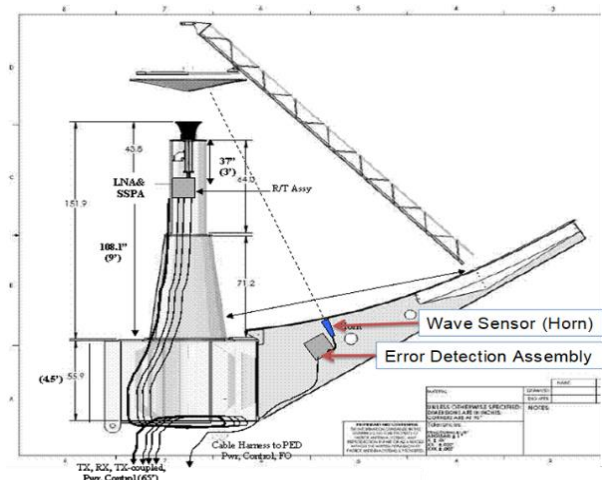


Fig. 14. Feedback point on antenna

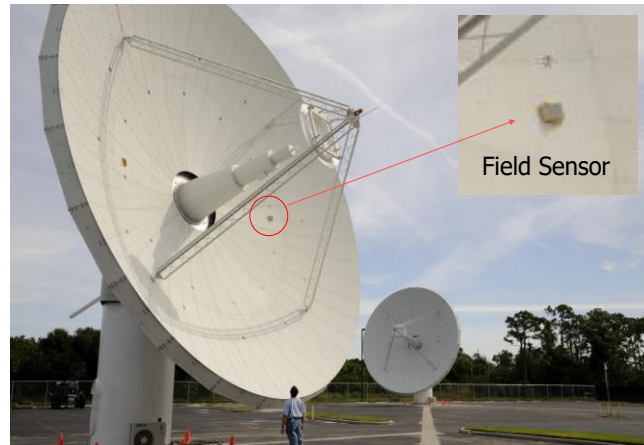


Fig. 15. Feedback sensor on reflector surface

Measured array performance for one of the numerous TxACE comm sessions is presented in Fig. 16. DISA permitted the TxACE array to use the DSCS-3 B13 geosynchronous satellite from time to time. B13 is significantly inclined, so even though it is at geostationary altitude, it appears to be continuously moving in a 'figure 8' relative to a point on the earth. The allocated satellite transponder was configured in a 'bent pipe' mode, sending back the uplink signal it received, thus providing measurement of array transmit performance. Although it would have been possible to track B13 using AOA, array pointing was calculated 'blindly' using TLE files provided by DISA.

Graphs labeled 1 and 2 on Fig. 16 are respectively elevation and azimuth from the array to the satellite. During the 3+ hour session, elevation varied 2 degrees and azimuth 4. At the 8.4 GHz frequency, element beamwidth is about 3 milliradians, about 0.17 degrees. So, the apparent motion was about 27 beamwidths over about three hours. Graph 5 is the ideal geometry based steering vector phase for elements 2 (cyan) and 3 (magenta) with respect to dish 1. As evidenced by graphs 8 and 9, respectively a single receive element signal and optimum array output signal, uplink performance was ideal over the experiment interval. In order that the ideal steering vector phasing actually produce an optimum transmit beam, it was necessary to compensate for circuitry variation. Graph 3 shows the circuit error being continually corrected by the Self-Controlled phase lock system, cyan and magenta respectively for dishes 2 and 3 with respect to dish 1. Notice that the scale is +/- 200 degrees (400 total). Nearly 180 degrees circuit phase variation was corrected between dishes 3 and 1, and more than 90 degrees between 2 and 1.

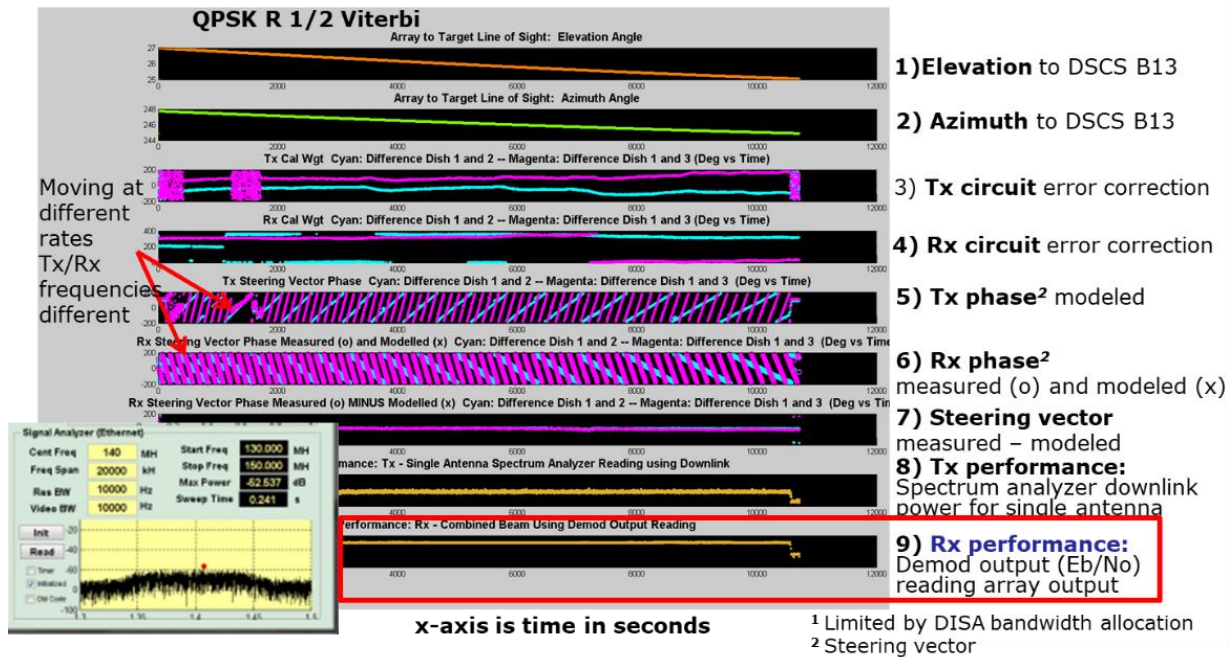


Fig. 16. 100% Self-Controlled arraying: Over a three-hour using 3-12m transmit reflector antennas to a GEO satellite arraying performance was ideal as seen in graphs 8 and 9. During a 10-month period in 2010-11, each time the system was powered up, optimal performance was demonstrated. No calibration was ever required using satellite feedback.

Receive array steering vector phase is graphed in line 6, with the colors again respectively depicting phase between a reflector and reflector 1. Actually, two sets of steering vectors are overlaid – the ideal geometry based steering vector and the measured receive steering vector. The small differences (less than 10 degrees) are due to propagation disturbances. During this particular run, no effort was made to compensate by pre-correcting the uplink.

6.3. Propagation media variation

Water, ice, water vapor and turbulence in the atmosphere, mostly in the troposphere, affect wave propagation. With array elements widely separated (thousands of wavelengths), different atmospheric effects are present in the different signal pathways. S-band is only slightly affected, but the effect is linearly proportional to frequency so three degrees phase variation at S band is 30 degrees at Ka. During weather events at X-band, we measured more than 26 degrees phase differentials. Without mitigation, these errors would be serious for beam formation and AOA accuracy. If a known location signal source (at a different frequency) is present in the array element's main beam, then it can be used to measure

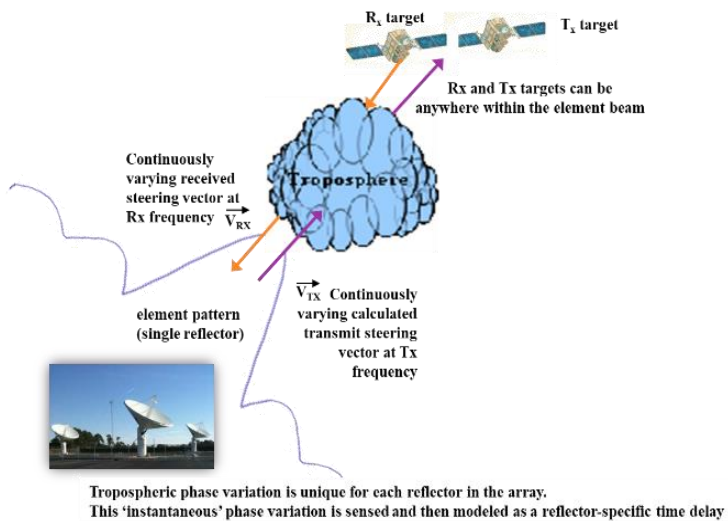


Fig. 17. Real-Time Tropospheric Variation Mitigation

the propagation effect. A radar or comm array application focused on the equatorial arc will be able to see many beacons and downlinks which could be used for this purpose. (Fig. 17)

On September 30, 2010, a run was conducted during a tropical depression. Weather satellite water vapor images, showed a large mass of humid air between the array and B13. (Fig. 18)

During the run, tropospheric propagation correction was turned on and off repeatedly, allowing a performance comparison. Fig. 19 shows a portion of the run. The top trace graphs the phase difference between measured and modeled receive steering vectors (representing the propagation error), with the colors as described before. A maximum difference reaching 27 degrees between reflectors 1 and 3 and 26 degrees between 1 and 2 was measured. The

lowest trace on the graph is output from the modem connected to the continuously optimized receive array output (this optimization of downlink signal is not affected by activation of uplink compensation). The x axis is time in seconds. From 100 seconds to about 310 seconds (the vertical red line), transmit adaptive pre-compensation (called 'Instant Return') is OFF. During that time uplink performance varied 2.2dB due to the propagation disturbance. With compensation ON, the maximum variation was 0.6dB, demonstrating the effectiveness of the process.

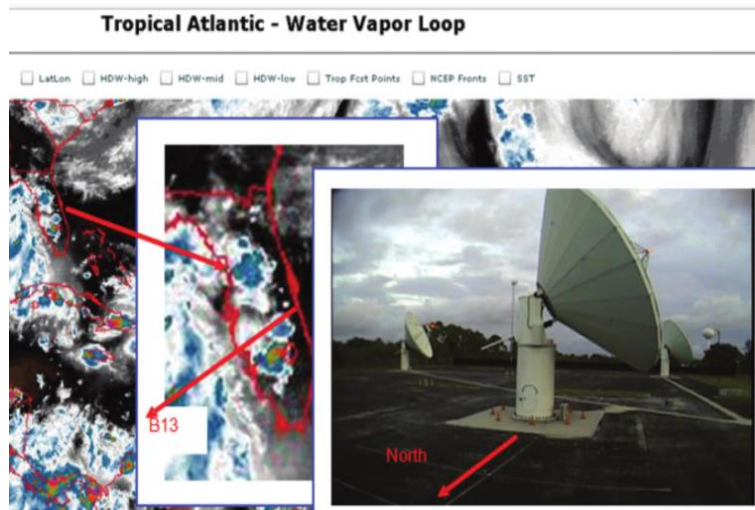


Fig. 18. Tropical Depression in Florida enables opportunity to test real-time Tropospheric mitigation at X-band; antennas 60m apart

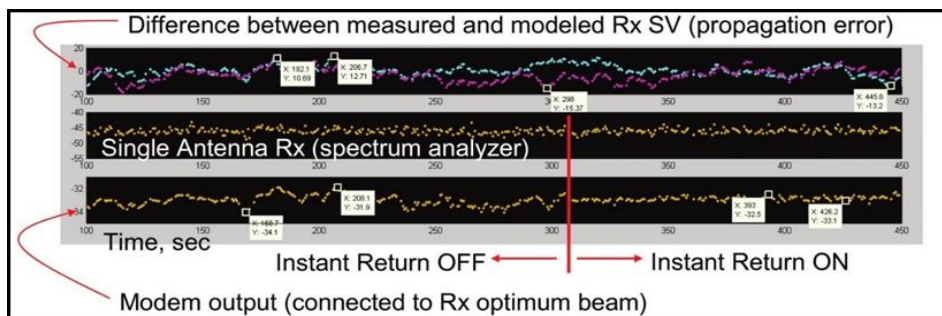


Fig. 19. Self-Controlled arraying demo, real-time tropospheric mitigation was made possible in a Tropical Depression because the receive and transmit arrays were each independently under a 100% phase lock. Remaining tropospheric errors were isolated and mitigated. With the Externally-Controlled arraying method this correction is not feasible.

Over the ten months period the TxACE array was operational, performance loss from ideal for all errors was less than 0.2dB. On one occasion immediately before a demonstration, an HPA failed. It was temporarily replaced by a component of different design and specification, and the array was instantly up and calibrated.

Operation of the TxACE array was witnessed on numerous occasions by representatives from APL, MIT-LL, and NASA (HQ, JSC, and Glenn).

7. History of reflector arraying experiments

Interest in widely-spaced element array transmit combining has persisted for decades but did not begin in earnest until about 2003. The need for a next-generation resilient COMM system for the Deep Space Network, DSN, was acknowledged at a time when the three 70m globally-spaced antennas were single-point failures; if one were to go down, 24/7 coverage could be lost and a space craft with a problem could be forever lost. In August 2006, the 70m antenna at Madrid was out of service about six months for azimuth bearing replacement [19]. While an interim solution had been implemented using several 34m beam waveguide reflectors, the clear future need for large reconfigurable arrays of reflectors supporting both transmit and receive capability remained.

At that time, NASA HQ recognized that widely spaced reflector transmit arraying was key, and advocated advancing this technology. Two different approaches, each with modeling and simulation support as well as successful demonstrations of critical aspects of their technology emerged. Three demonstrations were funded between 2008 and 2010, establishing the fundamental properties of the two approaches. Two of these demonstrations were conducted by JPL, both relying upon the Externally-Controlled method, while the third demonstration referred to as TxACE (Transmit Adaptive Combining Experiment) was based upon an entirely different calibration method, a locally Self-Controlled arraying method, which maintains calibration indefinitely without needing recalibration.

7.1.1 JPL Two-antenna Swept Phase (Vilnrotter)

2006: Using two 34m DSN beam waveguide antennas pointed to the EPOXI satellite at X-band, the transmit phase of one was slowly swept versus the other resulting in a maximum when the variable phasing passed through the correct value. Signal strength monitoring information onboard the satellite was downlinked to report performance. This experiment showed that the widely spaced DSN antennas and associated electronics were stable enough for beam formation over a short period. Restriction to two elements is necessary due to the difficulty of simultaneously satisfying degrees of freedom constraints.

7.1.2 JPL Moon Bounce (Vilnrotter, et al)

2007: Following the Swept Phase experiment success, JPL subsequently attempted a three DSN reflector uplink experiment. Even with stable hardware, there are unknown phase differences between the antennas, due primarily to circuitry, which must be resolved (calibrated) in order to coherently combine the three antennas. Vilnrotter and the team solved this problem using ISAR imaging of a far-field object, the moon [20]. Because the entire moon is too large with too great differential time delay variation, the imaging was restricted to Tycho Crater. Images were formed pairwise between DSN 34m antennas, each requiring about 30 minutes to complete, and yielded a measure of residual differential phase errors (the calibration). With the differential phase errors corrected, the antennas were then used to communicate with the EPOXI satellite, verifying coherent beam formation.

7.1.3 JPL Calibration Towers (D'Addario, Larry et al)

2009: In an alternate uplink array design concept, D'Addario envisioned a larger array of smaller reflectors [21]. With this approach, a calibration tower in the far-field of the smaller reflectors would obviate the need for a very distant far-field object, such as the moon or a dedicated calibration satellite. This design used five closely spaced 1.2m antennas in a linear array operating at Ku-band to commercial satellites. An advanced time-transfer method was used to help synchronize the antennas, with an external calibration tower providing information enabling solution for element-dependent unknown phase including filters, antenna feed, and internal reflector variations.

7.1.4 NASA TxACE (Martin & Minear)

2010: The only government-funded, industry led arraying demonstration did not use the Externally-Controlled arraying method. [6]. It used the Self-Controlled method on three 12 m antennas that were spaced about 60 m apart and communicated at X-band with a GEO satellite. Precise transmit and receive arraying were demonstrated, including real-time tropospheric mitigation. The array remained coherent for the entire ten months of operation before being delivered to KSC.

7.15 KaBOOM (KSC, JPL)

2012-15: The three 12m antennas used during the TxACE program were moved to KSC in 2012. These were intended for developmental use at Ka-band, however Ka-BOOM and KARNAC were X-band arraying experiment. Led by JPL and KSC, they reverted to a variation of the JPL Calibration Tower method using GEO satellites. This program ended in 2016 without transitioning to Ka-Band [22].

7.1.6 ASRE (APL, JPL, et al)

2017: Jet Propulsion Lab, SRI, GBO, Aerospace, MITRE, MIT Lincoln Laboratory, and JHU/APL participated in an arraying experiment that used the three Deep Space Network, 34m antennas [23]. It was called the Advanced Space Radar Experiment (ASRE). It demonstrated that arrayed signals could be bounced off commercial satellites and received at the Allen Telescope Array (ATA). However, no report can be found in the public domain regarding the quality of the arrayed beam at the target; whether it formed at the target of interest or was spread in the local region around the target.

7.1.7 DARC (JPL, APL)

Space Force's Deep Space Advanced Radar Concept (DARC) is a ground-based, SDA radar system to detect, track, and maintain custody of deep space objects 24/7. (Air Force DoD 2022 budget estimates) [24]. The three global sites are expected to cost over \$1B. Each site is anticipated to contain 10-15 receive and 4-6 transmit reflectors.

Widely-spaced reflector antenna arraying is the enabling technology for DARC. Competition for the arraying method was ongoing since 2017 and was only open to government labs, JHU/APL and JPL and others. Northrup Grumman won the contract for the first site in March of 2022 with the arraying technology transferred from APL. Northrup is expected to deliver site one by 2025.

8. Arraying method performance metrics, N^2 EIRP

It is not enough to be satisfied with detectable radar returned pulses or, in a comm system, the ability to communicate, as this conveys little information about beam quality and whether the antennas are properly phased; a badly formed beam with multiple lobes away from the target can still have enough power on the target to return a detectable pulse or communicate with a spacecraft.

With 'unlimited' time, pairwise sum and difference excitation of the array elements can validate proper beamforming, provided the reflectors are accurately pointed toward the target. Then groups of elements can be combined similarly. With even more time, the beam can be scanned past the target, confirming shape and EIRP. However, this level of detail is not practical for operational systems.

A fast and reliable test is for EIRP increase proportional to N^2 , $EIRP_{dB} \propto 20\log_{10}(N)$, assuming 'equal' antennas. With a 24/7/365 system, this can be implemented by bringing one antenna up, then two, then four, then eight, and so on. With each doubling, EIRP must increase by 6dB. For three antennas this is a 9.54 dB increase.

In between satellite test periods, if the arraying method is robust, the array should remain calibrated, so simply turning it on should show this result. If the array does not pass this EIRP test, then calibration has changed and a detailed investigation is required.

The Self-Controlled method was tested with the N^2 EIRP method over a 10-month period on NASA TxACE with less than 0.2dB loss over theoretical, 9.54dB.

N^2 EIRP test is recommended as a performance metric for all arraying methodologies. Testing should occur over months, using at least three antennas and with spacing commensurate with the largest diameter of the completed array.

9. Conclusion

Today's orbital debris cataloging systems are inadequate; particularly for the estimated million 1 - 10 cm objects at altitudes from LEO, < 2000 km, to GEO at 36,250 km. The highest density of debris in this range are particles 1 - 2cm. These pose the greatest risk to space assets and astronauts.

One problem with today's systems is that they operate at S-band or lower frequencies and/or they lack the high EIRP and sensitivity required to see and characterize particles in higher orbits. Even S-band Space Fence is limited to objects > 10 cm, and has coverage mostly in LEO using a fan-beam, though it can combine its energy to reach MEO.

A notional solution to these 1-10 cm threats is an X-band array of reflector antennas, equipped with the "Self-Controlled" arraying technology, with real-time tropospheric mitigation signal processing. A compact transmit array coupled with a wide diameter receive array, both arrays with 100% phased lock arraying technology could enable very high precision orbit determination and, at X band, cataloging of objects as small as 1 cm in GEO

"Self-Controlled" arraying technology is already at a technical readiness level, TRL-7. It was invented and successfully demonstrated by the authors at X-band in comm mode to a GEO satellite on NASA funding. Both transmit and receive arrays remained optimally coherent (< 0.2dB loss) using the N^2 performance metric for the entire 10-month period of operations, never needing calibrating. It successfully demonstrated tropospheric scintillation mitigation during a tropical depression. Exceptional Engineering Achievement medals were awarded by NASA HQ for the achievement in 2011. Tropospheric scintillation mitigation may be necessary for X-band operation and definitely for Ka-band.

The two distinct arraying methods were discussed, Self-Controlled and Externally-Controlled. The Self-Controlled arraying method never requires far-field (satellite) objects for antenna and circuitry phasing errors making it the most reliable 24/7/365 system for tomorrow's Deep Space communications and radar missions.

It was shown how the Externally-Controlled arraying method began with a 2003 JPL paper incorrectly asserting that a far-field object was the only way to account for antenna and circuitry phasing errors among the antennas and how that notion influenced arraying demonstrations until today.

10. References

- [1] European Space Agency. (2022, 08 11). *Space Safety*. Retrieved from The European Space Agency: https://www.esa.int/Space_Safety/Space_Debris/Space_debris_by_the_numbers
- [2] Undseth, M., C. Jolly and M. Olivari (2020), "Space sustainability: The economics of space debris in perspective", OECD Science, Technology and Industry Policy Papers, No. 87, OECD Publishing, Paris, <https://doi.org/10.1787/a339de43-en>.
- [3] NASA. (2021,05 27). *Space Debris and Human Spacecraft*. Retrieved from NASA: https://www.nasa.gov/mission_pages/station/news/orbital_debris.html
- [4] Johnson N. L., Krisko P.H., Liou J. C. Anz-Meador P. D. et al., (2001) *NASA's New Breakup Model of EVOLVE 4.0*, Advances in Space Research, Volume 28, Issue 9, Pages 1377-1384 [https://doi.org/10.1016/S0273-1177\(01\)00423-9](https://doi.org/10.1016/S0273-1177(01)00423-9), ISSN 0273-1177.
- [5] Martin G. P. Dr. and Minear, K. et al "*Large Reflector Uplink Arraying*", AIAA, Reston, Virginia, "Space Operations Exploration, Scientific Utilization, and Technology Development, Vol. 235, Ch. 24, 409-228, 2011.
- [6] Martin G. P. Dr. and Minear, K. et al, (2010 04) "*Large Reflector Uplink Arraying*", Proceedings of AIAA SpaceOps Conference, Huntsville, Alabama
- [7] Minear, K. and Martin G. P. (2018) "*System and Method for Detection and Orbit Determination of Earth Orbiting Objects*", U.S.P.O, Patent 9,989,634 Specialized Arrays Inc.
- [8] Acosta R., Nessel J. (2010) "*Path length fluctuations derived from site testing interferometer data.*" NASA Technical Memorandum 2010-216355.
- [9] Farid Amoozegar, Leslie Paal , James Layland, Robert Cesarone, Vahraz Jamnejad, Arnold Silva, Dave Losh, Bruce Conroy, Tim Cornish. (2003 11) "Uplink Array System of Large or Small Aperture Antennas for the Deep Space Network; Calibration and Testbed", Jet Propulsion Laboratory California Institute of Technology Pasadena
- [10] Martin G. P. Dr. and Minear, K. et al "*Large Reflector Uplink Arraying*", AIAA, Reston, Virginia, "Space Operations Exploration, Scientific Utilization, and Technology Development, Vol. 235, Ch. 24, 409-228, 2011.
- [11] D'Addario, L., Proctor, R., Trinh, J., Sigman, E., and Yamamoto, C., (2009 02 15) "*Uplink Array Demonstration with Ground-Based Calibration,*" Interplanetary Network Progress Report, Vol. 42-176, Jet Propulsion Lab., Pasadena, CA.
- [12] Davarian, F. (2008 11 15) "*Uplink Arraying Next Steps,*" Interplanetary Network Progress Report Vol. 42-175, Jet Propulsion Lab., Pasadena, CA. https://ipnpr.jpl.nasa.gov/progress_report/42-175/175C.pdf
- [13] Specialized Arrays. (2020) *Deep Space COMM*. Retrieved from SARRAYS: <https://sarrays.com/what-we-do/deep-space-comm/>
- [14] J. A. Nessel and R. J. Acosta, (2010) "*Atmospheric compensation for uplink arrays via radiometry,*" 2010 IEEE Antennas and Propagation Society International Symposium, pp. 1-4, doi: 10.1109/APS.2010.5561705

- [15] Martin N. (2022 03 25) “*APL Delivers New Satellite Tracking Capability for USSF*”, Retrieved from Executive Gov: <https://executivegov.com/2022/03/jhu-apl-develops-space-object-tracking-tech-for-ussf/>
- [16] Global Security.org. (2022) “*Deep Space Advanced Radar Capability – DARC.*” Retrieved from Global Security: <https://www.globalsecurity.org/space/systems/darc.htm>
- [17] Erwin S., (2022 02 23) “*Northrop Grumman wins \$341 million Space Force contract to develop a deep-space tracking radar.*” Retrieved from Space News: <https://spacenews.com/northrop-grumman-wins-341-million-space-force-contract-to-develop-a-deep-space-tracking-radar/>
- [18] Geldzahler B. et al, (2017) “*A phased array of widely separated antennas for space communications and planetary radar,*” Advanced Maui Optical and Space Surveillance Technologies Conference, Retrieved from AMOS Tech: <https://amostech.com/TechnicalPapers/2017/Poster/Geldzahler.pdf>
- [19] Chandler, David, (2006 08 02) “*Key antenna failure threatens Deep Space Network.*” Retrieved from New Scientist: [Key antenna failure threatens Deep Space Network | New Scientist](#)
- [20] Vilnrotter, V., Lee, D., Mukai, R., Cornish, T., and Tsao, P., (2007 05 15) “*Three-Antenna Doppler-Delay Imaging of the Crater Tycho for Uplink Array Calibration Applications,*” Jet Propulsion Lab., Pasadena, CA, The Interplanetary Network Progress Report, Vol. 42-169, pp 1-17.
- [21] D’Addario, L., Proctor, R., Trinh, J., Sigman, E., and Yamamoto, C., (2009 02 15) “*Uplink Array Demonstration with Ground-Based Calibration,*” Jet Propulsion Lab., Pasadena, CA, Interplanetary Network Progress Report, Vol. 42-176.
- [22] Geldzahler, et. al., “*A Phased Array of Widely Separated Antennas for Space Communication and Planetary Radar*”, (2017 09, Advanced Maui Optical and Space Surveillance Technologies Conference.
- [23] Green Bank Observatory, (2017 07 10) “*GBT Joins Goldstone and Allen Telescope Array in Radar Test,*” Retrieved from: Green Bank Observatory, The Observer – Volume I, Issue 3.
- [24] Air Force, (2021 05), “*Department of Defense Fiscal Year (FY) 2022 Budget Estimates*”, Justification Book Volume 1 of 1, Research, Development, Test & Evaluation, Space Force.